Subcutaneous Adipose Tissue and Systemic Inflammation Are Associated With Peripheral but Not Hepatic Insulin Resistance in Humans

Subcutaneous Adipose Tissue and Systemic Inflammation Are Associated With Peripheral but Not Hepatic Insulin Resistance in Humans

Birgitta W. van der Kolk,[1] Marianthi Kalafati,[2,3] Michiel Adriaens,[3] Marleen M.J. van Greevenbroek,[4] Nicole Vogelzangs,[3,5] Wim H.M. Saris,[1] Arne Astrup,[6] Armand Valsesia,[7] Dominique Langin,[8,9,10] Carla J.H. van der Kallen,[4] Simone J.P.M. Eussen,[5] Casper G. Schalkwijk,[4] Coen D.A. Stehouwer,[4] Gijs H. Goossens,[1] Ilja C.W. Arts,[3,5] Johan W.E. Jocken,[1] Chris T. Evelo,[2,3] and Ellen E. Blaak[1]

Diabetes 2019;68:2247–2258 | https://doi.org/10.2337/db19-0560

Obesity-related insulin resistance (IR) may develop in multiple organs, representing various etiologies for cardiometabolic diseases. We identified abdominal subcutaneous adipose tissue (ScAT) transcriptome profiles in liver or muscle IR by means of RNA sequencing in overweight or obese participants of the Diet, Obesity, and Genes (DiOGenes) (NCT00390637, ClinicalTrials.gov) cohort (n = 368). Tissue-specific IR phenotypes were derived from a 5-point oral glucose tolerance test. Hepatic and muscle IR were characterized by distinct abdominal ScAT transcriptome profiles. Genes related to extracellular remodeling were upregulated in individuals with primarily hepatic IR, while genes related to inflammation were upregulated in individuals with primarily muscle IR. In line with this, in two independent cohorts, the Cohort on Diabetes and Atherosclerosis Maastricht (CODAM) (n = 325) and the Maastricht Study (n = 685), an increased systemic low-grade inflammation profile was specifically related to muscle IR but not to liver IR. We propose that increased ScAT inflammatory gene expression may translate into an increased systemic inflammatory profile, linking ScAT inflammation to the muscle IR phenotype. These distinct IR phenotypes may provide leads for more personalized prevention of cardiometabolic diseases.

Worldwide, over 2.1 billion people were overweight or obese in 2013 (1). Overweight and obesity are major risk factors for type 2 diabetes (2,3). Adipose tissue dysfunction, rather than excess fat mass per se, is frequently associated with progression toward skeletal muscle, liver, and whole-body insulin resistance (IR) (4,5).

Adipose tissue dysfunction is characterized by increased adipocyte size (hypertrophy) rather than increased adipocyte number (hyperplasia) (6), and this seems to be associated with impairments in adipose tissue lipid buffering capacity (7). In addition, expanded adipose tissue mass is accompanied by an increased production and secretion of proinflammatory cytokines, chemokines, and adipokines (8,9). Both systemic lipid overflow and

[1]Department of Human Biology, NUTRIM School of Nutrition and Translational Research in Metabolism, Maastricht University, Maastricht, the Netherlands
[2]Department of Bioinformatics – BiGCaT, NUTRIM School of Nutrition and Translational Research in Metabolism, Maastricht University, Maastricht, the Netherlands
[3]Maastricht Centre for Systems Biology (MaCSBio), Maastricht University, Maastricht, the Netherlands
[4]Department of Internal Medicine, CARIM School for Cardiovascular Diseases, Maastricht University, Maastricht, the Netherlands
[5]Department of Epidemiology, CARIM School for Cardiovascular Diseases, Maastricht University, Maastricht, the Netherlands
[6]Department of Nutrition, Exercise and Sports, Faculty of Science, University of Copenhagen, Copenhagen, Denmark
[7]Nestlé Institute of Health Sciences, Lausanne, Switzerland
[8]INSERM, UMR1048, Institute of Metabolic and Cardiovascular Diseases, Toulouse, France
[9]Paul Sabatier University, Toulouse, France
[10]Laboratory of Clinical Biochemistry, Toulouse University Hospitals, Toulouse, France

Corresponding author: Ellen E. Blaak, e.blaak@maastrichtuniversity.nl

Received 6 June 2019 and accepted 27 August 2019

Clinical trial reg. no. NCT00390637, clinicaltrials.gov

This article contains Supplementary Data online at http://diabetes.diabetesjournals.org/lookup/suppl/doi:10.2337/db19-0560/-/DC1.

B.W.v.d.K. and M.K. share first authorship.

C.T.E. and E.E.B. share last authorship.

low-grade inflammation are thought to contribute to the development of IR in skeletal muscle and liver (10).

Whole-body IR reflects defective insulin action in major metabolic organs, such as skeletal muscle, liver, brain, and adipose tissue, and has long been known to precede the development of cardiometabolic diseases (10). IR can develop simultaneously in multiple organs, but the severity may vary between organs. For instance, impaired fasting glucose and impaired glucose tolerance may represent distinct prediabetic phenotypes, which are characterized by more pronounced hepatic or muscle IR, respectively (11). In line with this, altered skeletal muscle fatty acid handling as well as more pronounced peripheral IR have been observed in individuals with impaired glucose tolerance compared with individuals with impaired fasting glucose (12,13). Moreover, the severity of IR at the tissue level may contribute to the differential response to lifestyle and pharmacological interventions. Indeed, physical activity has been shown to mainly target skeletal muscle insulin sensitivity (14), while metformin treatment might have more pronounced effects on hepatic insulin sensitivity (15). Moreover, a low-fat, high–complex carbohydrate diet may result in a more pronounced increase in the disposition index in individuals with prediabetes with hepatic IR, while a Mediterranean diet may have more beneficial effects in individuals with muscle IR (16).

Analysis of gene expression in subcutaneous adipose tissue (ScAT) may help to elucidate the pathways and mechanisms that link adipose tissue function to tissue-specific IR. Previous studies have shown significant dysregulation in the ScAT transcriptome in obesity and IR (17). For instance, Elbein et al. (18) found that ScAT inflammatory and cell cycle–regulatory pathways were upregulated in individuals with whole-body IR compared with insulin-sensitive BMI-matched individuals, while lipid metabolism pathways were downregulated. In addition, Soronen et al. (19) observed upregulation of inflammatory pathways and downregulation of mitochondrial respiratory and lipid metabolism pathways in obese women with whole-body IR. In addition, recent transcriptome analyses of abdominal ScAT during weight loss in individuals from the Diet, Obesity, and Genes (DiOGenes) study highlighted the link between lipid metabolism pathways and glycemic improvement (20).

Studies that focus on detailed characterization of tissue-specific IR phenotypes are scarce, and it is currently not known whether differential ScAT transcriptome profiles are related to more pronounced muscle or hepatic IR. Identification and quantification of metabolic anomalies in various IR phenotypes may provide direction for more personalized lifestyle or pharmacological interventions in the prevention and control of cardiometabolic diseases. Here, we studied the ScAT transcriptome of overweight and obese participants without diabetes from the DiOGenes study (21), a large European multicenter dietary intervention study. We analyzed baseline RNA sequencing data in abdominal ScAT from 368 individuals and identified gene clusters that were associated with muscle or hepatic IR. Subsequently, we investigated whether we could confirm mechanisms suggested by ScAT transcriptome findings by performing complementary analyses on systemic inflammatory profiles in two independent human cohorts, namely, CODAM (Cohort on Diabetes and Atherosclerosis Maastricht) (22) and the Maastricht Study (23).

RESEARCH DESIGN AND METHODS

Study Design

DiOGenes is a multicenter, randomized, controlled dietary intervention study that involved eight European countries. Briefly, 938 overweight or obese adults without diabetes (age 18–65 years, BMI 27–45 kg/m^2, and blood fasting glucose $<$6.1 mmol/L) were included. More details about this study have been described previously (21). For current analyses, baseline data were used of 368 participants for whom abdominal ScAT RNA sequencing and oral glucose tolerance test (OGTT) data were available.

CODAM is a prospective, observational study on, among other things, the natural progression of IR and glucose tolerance. A total of 574 individuals (aged $>$40 years) were included from a large population-based cohort, as previously described in detail (22). The Maastricht Study is a large population-based cohort (participants aged 40–75 years) that is enriched with participants with type 2 diabetes and that focuses on the etiology of type 2 diabetes, its classic complications, and its emerging comorbidities (23). The analyses described here include the baseline data of 325 CODAM (BMI $>$25 kg/m^2) and 685 Maastricht Study (BMI $>$27 kg/m^2) overweight/obese participants without diabetes for whom data on OGTT and systemic low-grade inflammation were available.

For the multicenter DiOGenes study, the protocol was approved by the ethics committee of each center/country. The DiOGenes study in Maastricht as well as CODAM and the Maastricht Study were approved by the local institutional medical ethics committee (Maastricht University Medical Center+), and the Maastricht Study was also approved by the Minister of Health, Welfare and Sports of the Netherlands (permit 131088-105234-PG). All participants gave written informed consent. These studies were carried out in accordance with the principles of the Declaration of Helsinki.

Estimates of Tissue-Specific IR and Classification of IR Subgroups

DiOGenes participants underwent a 5-point OGTT at baseline. In short, after an overnight fast, venous blood was sampled at baseline and after a 75-g flavored glucose load was ingested. Blood samples were taken at 0, 30, 60, 90, and 120 min, and plasma was stored at −80°C until analysis to determine glucose and insulin concentrations. CODAM participants underwent a 4-point OGTT with blood samples taken at 0, 30, 60, and 120 min. The Maastricht Study participants underwent a 7-point OGTT with blood samples taken at 0, 15, 30, 45, 60, 90, and 120 min. Muscle insulin sensitivity and hepatic IR were estimated using the methods of Abdul-Ghani et al. (24).

The muscle insulin sensitivity index (MISI) was calculated according to the following formula: MISI = (dG/dt)/mean plasma insulin concentration during OGTT. Here, dG/dt is the rate of decay of plasma glucose concentration during the OGTT, calculated as the slope of the least square fit to the decline in plasma glucose concentration from peak to nadir (24). The decline in plasma glucose concentration in the second part of the OGTT primarily reflects glucose uptake by peripheral tissues, mainly skeletal muscle. This index has been developed and validated against measures of peripheral insulin sensitivity as assessed during a hyperinsulinemic-euglycemic clamp using a stable isotope glucose tracer (24).

The hepatic IR index (HIRI) was calculated using the square root of the product of the areas under the curve (AUCs) for glucose and insulin during the first 30 min of the OGTT, i.e., sqrt(glucose 0–30 [AUC in mg/dL*h] * insulin 0–30 [AUC in μU/mL*h]). This index has been developed and validated against the product of fasting plasma insulin and endogenous glucose production during a hyperinsulinemic-euglycemic clamp using a stable isotope glucose tracer (24).

DiOGenes, CODAM, and Maastricht Study participants were each divided into four groups based on the tertiles of HIRI and MISI scores for each cohort (16). The lowest tertile of MISI represented individuals with muscle IR; the highest tertile of HIRI represented individuals with hepatic IR. Accordingly, participants were categorized into one of four groups: *1*) no IR, *2*) IR primarily in muscle (muscle IR), *3*) IR primarily in liver (liver IR), and *4*) IR in both muscle and liver (muscle/liver IR).

Adipose Tissue Biopsy, RNA Preparation, and RNA Sequencing

In DiOGenes, needle biopsies of abdominal ScAT were performed 6–8 cm lateral to the umbilicus under local anesthesia; the biopsy specimens were snap-frozen in liquid nitrogen and stored at −80°C until analysis. Total RNA was extracted from these abdominal ScAT specimens as previously described (25). For each sample, we used GenomicAlignments to retrieve the number of reads mapping onto 53,343 genes (GRCh37 assembly). Only reads with both ends mapping onto a single gene were considered.

Statistical Analyses

Participant Characteristics

In DiOGenes, CODAM, and the Maastricht Study, descriptive variables with a skewed distribution were $\log_e$-transformed before further analyses. The phenotypic differences between tissue-specific IR groups were assessed using one-way ANOVA for continuous variables with Bonferroni post hoc tests, adjusted for sex, and χ^2 test for categorical variables. The threshold for statistical significance was set at $P < 0.05$.

Differential RNA Expression Analyses

In DiOGenes, after alignment and determination of transcript abundance, we analyzed estimated raw count data for 53,343 genes and 368 samples in RStudio software (version 3.2). Differential expression analysis was performed in the DESeq2 package (version 1.12.4) using default settings (26). Prefiltering of genes with low counts was applied by removing genes with a total of zero reads or one read. The standard differential expression analysis steps are wrapped into a single function, *DESeq* (26). The differential expression analysis in DESeq2 implements a negative binomial generalized linear model with the tissue-specific IR phenotypes (muscle IR, liver IR, and no IR), study center, sex, BMI, and waist-to-hip ratio as covariates. Due to a small number of men ($n = 12$) in the muscle IR group, we were not able to stratify our results by sex. The DESeq2 model internally corrects for library size; no additional data normalization was applied. The result tables were generated using the function *results* comparing the tissue-specific IR phenotypes (liver IR vs. no IR, muscle IR vs. no IR). Furthermore, the method *fpkm* was used from DESeq2 to calculate relative expression of transcripts. We obtained the transcript lengths using the Biostrings R package. The GRange transcript lengths were added to the DESeq object through the use of the rowRanges method. Then the *fpkm* method extracted the values for fragments per kilobase of transcript per million mapped reads.

In an additional analysis, including all participants, MISI and HIRI were simultaneously included as continuous independent variables in the model with gene expression as the dependent variable to assess their independent effects. To allow for direct comparison of the effect sizes, we also standardized β coefficients by calculating their *z* scores. Study center, sex, BMI, and waist-to-hip ratio were included as other covariates in the model.

Gene Ontology Analysis

Gene ontology (GO) analysis was performed using Gorilla software (27). Applied settings were *1*) organism, *Homo sapiens*; *2*) running mode, two unranked lists of genes (target and background lists); *3*) ontology, process; and *4*) $P < 0.05$. All significant genes (nominal $P < 0.05$) were included (Supplementary Tables 1 and 2) and divided into up- and downregulated genes to provide direction for the involved biological processes, and this gave four different sets of results. For each result, based on Benjamini and Hochberg false discovery rate *P* values, the top five biological processes were selected.

Pathway Analysis

Pathway analysis was performed with PathVisio 3.2.1. The curated human pathway collection was obtained from WikiPathways (version 20171116) (28), containing 344 pathways. An overrepresentation analysis was performed with the RNA sequencing data set. The pathways were then ranked based on a standardized difference score (*z* score). Pathways were considered significantly changed when *1*) *z* score was >1.96, *2*) permuted *P* was <0.05, and *3*) the pathway contained three or more significantly different genes (nominal $P < 0.05$).

Association With Low-Grade Inflammation Score

In CODAM and the Maastricht Study, linear regression analyses were performed with a low-grade inflammation score as the independent variable and HIRI or MISI (continuous variables) as the dependent variable (model 1). Skewed variables were $\log_e$-transformed. The low-grade inflammation score was calculated by averaging the *z* scores of eight inflammatory markers in CODAM (C-reactive protein [CRP], interleukin [IL]-6, IL-8, serum amyloid A [SAA], soluble intercellular adhesion molecule 1 [sICAM-1], tumor necrosis factor-α [TNF-α], ceruloplasmin, and haptoglobin) and six markers in the Maastricht Study (CRP, IL-6, IL-8, SAA, sICAM-1, TNF-α). Averaging these markers of low-grade inflammation produces a robust estimate of the overall inflammatory state with minimization of random error (29). To allow for direct comparison of the effect sizes, we also standardized HIRI and MISI by calculating their *z* scores. In model 2a, HIRI was included as a covariate in analyses on MISI, and vice versa, to assess the independent effects of tissue-specific IR, and in model 2b, age, sex, BMI, and waist-to-hip ratio were included as covariates. Finally, in model 3, the covariates of model 2a and 2b were combined. All data were analyzed using SPSS for Mac version 24.0 (SPSS Inc., Chicago, IL) and R statistical programming language (version 3.3.3).

Data and Resource Availability

RNA expression data are available from the Gene Expression Omnibus under accession no. GSE95640 (20). Other data are unsuitable for public deposition due to ethical restrictions and privacy of participant data. Data are available from the corresponding author for any interested researcher who meets the criteria for access to confidential data and upon reasonable request.

RESULTS

Characteristics of the DiOGenes Population

Table 1 shows the demographic and metabolic characteristics of the DiOGenes participants according to their tissue-specific IR phenotype. In the no-IR group, 68% of participants were women. Participants in the liver-IR group were less often women (47%; $P = 0.006$), while participants with muscle IR were more often women (82%; $P = 0.027$). Comparisons of other characteristics between groups were adjusted for sex. Participants in the muscle/liver-IR group had significantly larger waist circumference and waist-to-hip ratio than those in the no-IR group. The muscle/liver-IR group also had significantly larger waist circumference, larger waist-to-hip ratio, and higher systolic blood pressure than the muscle-IR group. Plasma triacylglycerol concentrations were significantly higher in the liver-IR and muscle/liver-IR groups than in those with no IR. Cholesterol concentrations were highest in participants in the liver-IR group, while HDL cholesterol was lowest in the muscle/liver-IR group. Concentrations of the inflammatory marker CRP were significantly higher in the participants in the muscle/liver-IR group than in those with no IR. Insulin concentrations were significantly higher in all groups than in the no IR group. Previous studies have shown similar characteristics for the various tissue-specific IR groups (16).

Extracellular Structure Organization Is Differentially Regulated in the Liver-IR and No-IR Groups

We performed RNA sequencing on the abdominal ScAT to assess transcriptome differences in adipose tissue in individuals with liver IR or muscle IR. The no-IR group was used as reference, and the analyses were adjusted for study center, sex, BMI, and waist-to-hip ratio. To gain insight into the differentially expressed transcriptome in the tissue-specific IR phenotypes, we performed GO enrichment analyses focusing on biological processes. We identified 2,416 genes that were differentially expressed in the liver-IR versus no-IR comparison (nominal $P < 0.05$), with in total 1,221 upregulated and 1,195 downregulated genes (Fig. 1 and Supplementary Table 1). The GO classifications with the strongest statistical significance for the upregulated genes was "extracellular structure organization" (including genes related to collagens, integrins, lamininis, and thrombospondins) and "mitotic cell cycle process" (including genes related to cell division cycle and kinesins) (Table 2 and Supplementary Table 5). In additional analyses in which adipose tissue gene expression was the dependent variable, continuous HIRI was the independent variable, and adjustments were made for study center, sex, BMI, waist-to-hip ratio, and MISI, similar significant associated genes (Supplementary Table 9) and GO terms (Supplementary Table 11) were found.

Subsequently, we included a pathway enrichment analysis using the WikiPathways human collection of curated pathways. Eight significantly different pathways were overrepresented in the liver-IR versus no-IR comparison, with at least one gene with absolute fold change >1.2 and genes with nominal $P < 0.05$ (Supplementary Table 7). Pathways related to extracellular matrix (ECM) organization (e.g., focal adhesion pathways) and mitotic cell cycle (e.g., cell cycle) were among the most significantly differing pathways in the comparison of the liver-IR and no-IR groups (Figs. 2 and 3).

In the comparisons of both the liver-IR and muscle-IR groups with the no-IR group, the GO classification with the highest enrichment in downregulated genes was "regulation RNA metabolic process" (Supplementary Tables 3 and 4), which was accompanied by enrichment of upregulated genes in the "mitotic cell cycle process" (Table 2). These data might indicate gene-specific translational repression as a means of controlling the mitotic proteome, which may complement posttranslational mechanisms for inactivating protein function (30).

Inflammatory Pathways Are Differentially Regulated in the Muscle-IR and No-IR Groups

For the muscle-IR versus no-IR comparison, 3,716 genes were differentially expressed (nominal $P < 0.05$), of which

Table 1—Characteristics of DiOGenes participants

	No-IR (n = 186)	Muscle-IR (n = 69)	Liver-IR (n = 53)	Muscle/liver-IR (n = 60)	P
Female sex (%)	68	82	47	61	<0.001
Age (years)	42 ± 7	41 ± 6	42 ± 6	41 ± 6	0.684
BMI (kg/m^2)	33.9 ± 4.6	35.0 ± 4.3	34.7 ± 4.8	35.7 ± 4.4*	0.029
Waist (cm)	104.9 ± 12.2	105.6 ± 11.5	111.3 ± 11.4	112.6 ± 14.1*	0.001
Waist-to-hip ratio	0.91 ± 0.09	0.90 ± 0.08	0.96 ± 0.08	0.96 ± 0.10*#	0.018
SBP (mmHg)	123 ± 15	123 ± 12	128 ± 14	130 ± 11*	0.004
DBP (mmHg)	76 ± 11	77 ± 10	80 ± 9	79 ± 11	0.340
Fat-free mass (kg)	57.9 ± 13.7	56.3 ± 10.8	66.3 ± 13.9*	61.8 ± 10.8	0.019
Body fat (%)	39.1 ± 8.8	42.0 ± 6.3	36.3 ± 8.1	39.9 ± 8.0	0.153
Triacylglycerol (mmol/L)	1.2 ± 0.5	1.4 ± 0.6	1.6 ± 0.7*	1.5 ± 0.6*	<0.001
Cholesterol (mmol/L)	4.8 ± 1.0	4.8 ± 0.9	5.2 ± 1.0	5.0 ± 0.9	0.096
HDL (mmol/L)	1.3 ± 0.3	1.2 ± 0.3	1.2 ± 0.2	1.1 ± 0.3*	0.003
LDL (mmol/L)	3.0 ± 0.9	2.9 ± 0.8	3.3 ± 0.8	3.2 ± 0.8	0.165
NEFA (μmol/L)	656 ± 309	739 ± 415	734 ± 474	657 ± 318	0.201
CRP (mg/L)	2.6 (1.3–5.1)	3.8 (2.3–5.9)	2.9 (1.3–5.0)	4.7 (2.4–7.1)*	0.004
Glucose (mmol/L)	5.0 ± 0.6	5.0 ± 0.6	5.3 ± 0.5	5.2 ± 0.7	0.036
Insulin (mU/L)	6.8 (4.9–9.8)	9.4 (7.5–14.0)*	12.4 (9.8–17.2)*	17.1 (12.1–23.5)*#§	<0.001
MISI (AU)	0.07 (0.05–0.11)	0.02 (0.00–0.03)*§	0.05 (0.04–0.08)*#	0.02 (0.01–0.02)*§	<0.001
HIRI (AU)	26.0 ± 5.5	28.5 ± 5.0*§	43.2 ± 8.7*#	46.8 ± 12.0*#§	<0.001

Data are mean ± SD (for normally distributed variables), median (interquartile range) (for skewed variables), or percentage (for categorical variables). P values were obtained by using the Pearson χ^2 test for sex, and by ANOVA, adjusted for sex, for the other variables. Skewed variables were $\log_e$-transformed before analysis. In addition, Bonferroni post hoc tests were performed. AU, arbitrary units; DBP, diastolic blood pressure; NEFA, nonesterified fatty acids; SBP, systolic blood pressure. *$P < 0.05$ vs. the no-IR group; #$P < 0.05$ vs. the muscle-IR group; §$P < 0.05$ vs. the liver-IR group.

1,977 were upregulated and 1,739 were downregulated (Fig. 1 and Supplementary Table 2). ScAT of individuals with muscle IR was characterized by higher expression of inflammatory genes. The GO terms with the highest enrichment with upregulated genes in ScAT were "mitotic cell cycle process" (including genes related to cell division cycle and kinesins) (Table 2) and "immune system response" (including genes related to several complement factors and chemokine) (Table 2 and Supplementary Table 4). "Antigen processing and presentation" was highly statistically significant as well (including genes related to proteasome degradation and lysosomal cathepsins) (Table 2 and Supplementary Table 4). Like the GO enrichment analyses, WikiPathways-related inflammatory pathways (e.g., microglia pathogen phagocytosis, IL-1, and megakaryocytes in the obesity pathway and complement activation pathway) were predominant in the comparison of the muscle-IR and no-IR groups (Figs. 2 and 3 and Supplementary Table 8). In additional analyses in which the adipose tissue gene expression was the dependent variable and the continuous MISI was the independent variable, after adjusting for study center, sex, BMI, waist-to-hip ratio, and HIRI we found similar significantly associated genes (Supplementary Table 10) and GO terms (Supplementary Table 11). Thus, ScAT of individuals with muscle IR is characterized by increased expression of genes involved in chemotaxis, complement activation, and immune cell function related to lysosomal (e.g., cathepsins) and ubiquitin-proteasomal degradation.

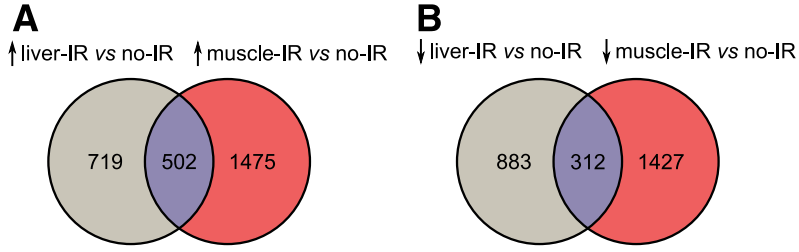

Figure 1—Venn diagrams of number of significantly upregulated (*A*) and downregulated (*B*) genes (nominal $P < 0.05$) in comparisons of the liver-IR and no-IR groups and of the muscle-IR and no-IR groups.

Table 2—GO analyses of differentially expressed genes in the liver-IR and muscle-IR groups compared with the no-IR groups in DiOGenes

Comparison	GO term	Description	FDR-*P*	Enrichment	Genes per GO term	
					Significant genes	Total genes
Liver-IR group vs. no-IR group						
Upregulated genes	GO:0043062	Extracellular structure organization	1.30E-07	3.34	40	270
	GO:0030198	ECM organization	2.31E-07	3.36	40	269
	GO:0007059	Chromosome segregation	2.07E-06	5.15	21	92
	GO:0051276	Chromosome organization	1.27E-04	2.52	41	367
	GO:1903047	Mitotic cell cycle process	1.46E-04	2.14	57	601
Downregulated genes	GO:0051252	Regulation of RNA metabolic process	1.26E-11	1.61	233	3,442
	GO:0016070	RNA metabolic process	1.54E-11	1.66	215	3,072
	GO:0006355	Regulation of transcription, DNA-templated	1.80E-11	1.62	222	3,245
	GO:2001141	Regulation of RNA biosynthetic process	2.56E-11	1.61	222	3,270
	GO:1903506	Regulation of nucleic acid–templated transcription	2.60E-11	1.62	222	3,264
Muscle-IR group vs. no-IR group						
Upregulated genes	GO:1903047	Mitotic cell cycle process	4.04E-14	2.36	111	601
	GO:0002376	Immune system process	4.73E-14	1.73	236	1,747
	GO:0019882	Antigen processing and presentation	3.73E-12	3.68	48	167
	GO:0022402	Cell cycle process	5.00E-12	1.95	145	949
	GO:0002478	Antigen processing and presentation of exogenous peptide antigen	2.72E-11	3.91	41	134
Downregulated genes	GO:0032774	RNA biosynthetic process	1.29E-15	1.73	251	2,349
	GO:0044260	Cellular macromolecule metabolic process	1.76E-15	1.36	518	6,161
	GO:0097659	Nucleic acid–templated transcription	2.89E-15	1.74	234	2,170
	GO:0006351	Transcription, DNA-templated	3.64E-15	1.74	234	2,169
	GO:0051252	Regulation of RNA metabolic process	7.35E-15	1.54	328	3,442

The top five most significant and biologically relevant GO biological processes are listed for the genes identified in Fig. 1*A* and *B*. False discovery rate *P* values (FDR-*P*) are presented for the GO analysis. Enrichment is defined as follows: (no. of significant genes in a specific GO term/no. of significant genes added to the GO analysis)/(total no. of genes associated with a specific GO term/total no. of identified genes).

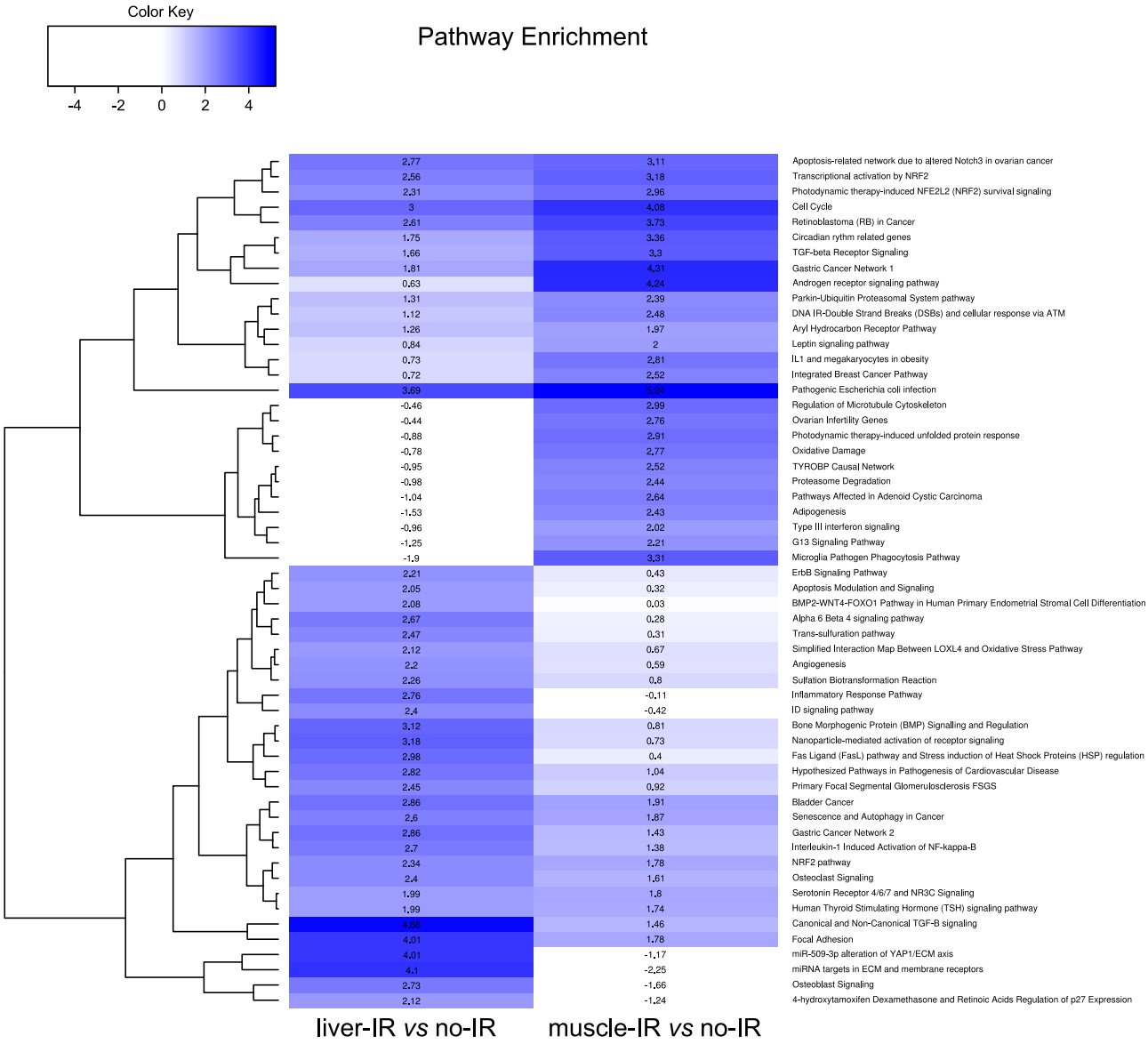

Figure 2—A heatmap representing the pathway enrichment analysis that applied the WikiPathways curated collection of human pathways. The pathways are ranked on the basis of a standardized difference score (*z* score). *z* scores >0 indicate enrichment for significantly different genes (blue gradients), and z scores <0 indicate an absence of enrichment for significantly different genes (white). Pathways were considered significantly different when *1*) *z* score was >1.96, *2*) permuted *P* was <0.05, and *3*) three or more significantly different genes (nominal $P < 0.05$) existed in the pathway. ECM, extracellular matrix; ID, inhibitor of DNA binding; NF, nuclear factor; TGF, transforming growth factor.

Systemic Low-Grade Inflammation Is Associated With Muscle IR in CODAM and the Maastricht Study

Following up on the transcriptome analyses, we hypothesized that increased ScAT inflammatory gene expression, as observed in the muscle-IR group, may lead to the secretion of proinflammatory adipokines in the circulation. Subsequently, a systemic proinflammatory profile may induce peripheral insulin sensitivity. As systemic inflammation markers were not available in DiOGenes, we studied the relationship between systemic inflammation and either muscle or liver IR in two independent cohorts, namely, CODAM and the Maastricht Study (22,23). In these cohorts, data on systemic low-grade inflammation and tissue-specific IR are available for 325 and 685 overweight/obese individuals without diabetes, respectively (Supplementary Tables 12 and 13). In general, participants in CODAM and the Maastricht Study had risk profiles for cardiometabolic diseases similar to those of DiOGenes participants but were less often women, slightly older, and less obese (Supplementary Table 14).

A combined score of several plasma markers of low-grade inflammation (which include adipose tissue–derived factors including, among others, IL-6, IL-8, TNF-α, SAA, sICAM, and CRP) was inversely associated with MISI in a linear

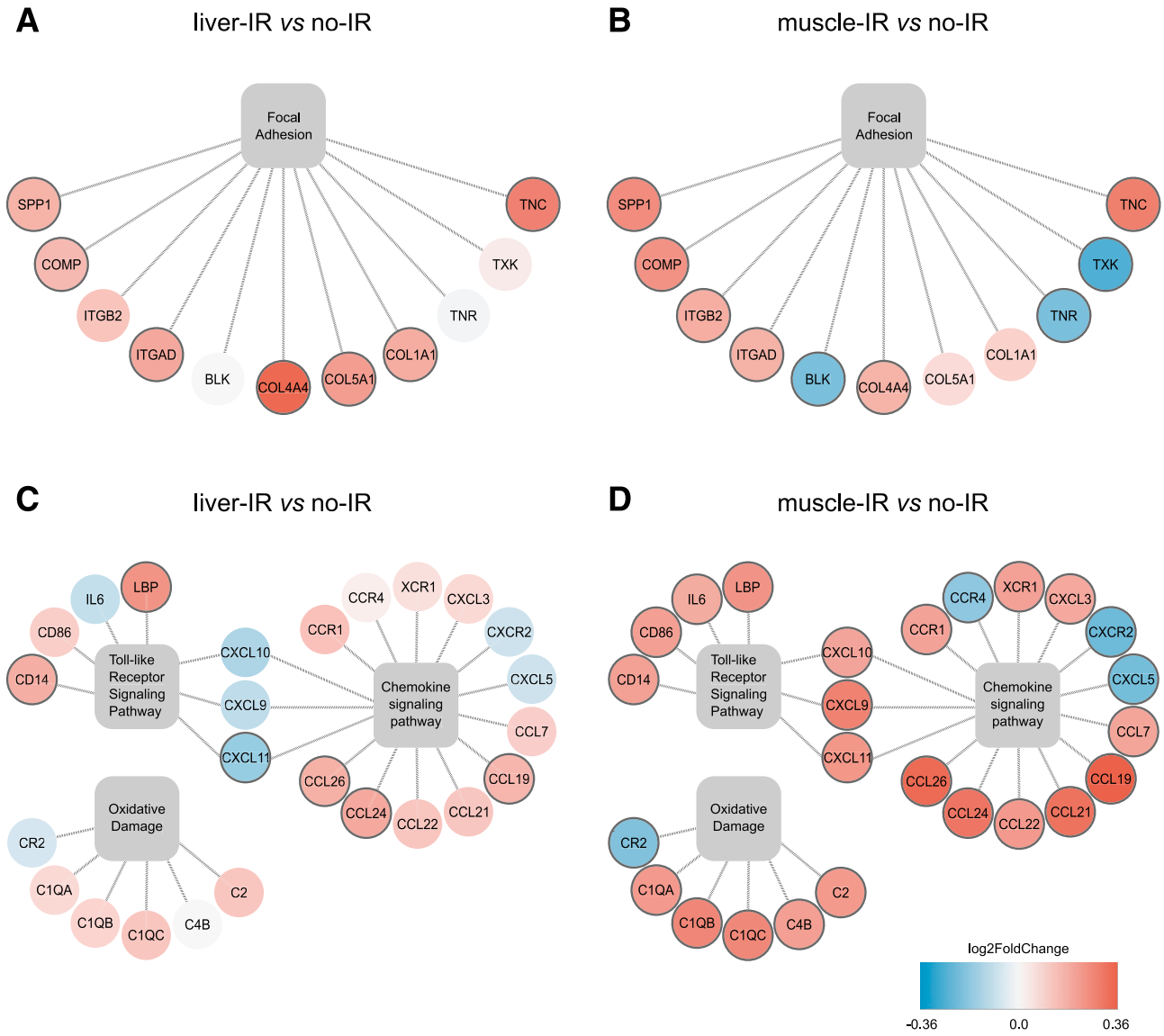

Figure 3—Four large pathways from the WikiPathways curated collection of human pathways, with comprehensive information on inflammation and extracellular matrix (ECM) remodeling, were selected and integrated into two networks. Visualizations were created for each network: two diagrams representing the ECM remodeling processes in the comparison between the liver-IR and no-IR groups (*A*) and the muscle-IR and no-IR groups (*B*), and two diagrams representing inflammatory processes in the comparison between the liver-IR and no-IR groups (*C*) and the muscle-IR and no-IR groups (*D*). Only genes with absolute fold change >1.1 and a nominal $P < 0.05$ for the liver-IR vs. no-IR comparison, the muscle-IR vs. no-IR comparison, or both were included. Pathway nodes are visualized as rounded rectangles and genes as circles; the colors are based on their fold change. Gradients of blue indicate downregulation, gradients of red indicate upregulation, and white represents unchanged genes. Genes that changed significantly (nominal $P < 0.05$) are indicated with a gray outline around the circle representing the particular gene.

regression analysis that was adjusted for HIRI (CODAM: standardized β [stdβ], −0.107 [$P = 0.028$]; Maastricht Study: stdß, −0.131 [$P < 0.001$]) (Table 3, model 2a). Notably, the low-grade inflammation score was not significantly associated with HIRI in a linear regression analysis that was adjusted for MISI (CODAM: stdß, 0.065 [$P = 0.184$]; Maastricht Study: stdß, 0.000 [$P = 0.995$]) (Table 3, model 2a). After additional adjustments for age, sex, BMI, and waist-to-hip ratio, the association between low-grade inflammation and MISI was maintained (CODAM: stdß, −0.051 [$P = 0.317$]; Maastricht Study: stdß, −0.091 [$P = 0.008$]) (Table 3, model 3). No significant sex interactions were observed for the associations between the low-grade inflammation score and MISI ($P_{interaction} = 0.639$) or HIRI ($P_{interaction} = 0.982$). Therefore, associations between low-grade inflammation and MISI or HIRI were assessed in men and women combined.

Finally, additional analyses in DiOGenes showed that in adipose tissue the RNA expression levels of seven out of

Table 3—Associations of plasma low-grade inflammation with MISI and HIRI

	CODAM, BMI >25 kg/m^2 (n = 325)			The Maastricht Study, BMI >27 kg/m^2 (n = 685)		
Model	β	LGI* (95% CI)	*P*	β	LGI# (95% CI)	*P*
MISI						
1	−0.180	−0.291 to −0.073	<0.001	−0.183	−0.257 to −0.109	<0.001
2a	−0.107	−0.205 to −0.011	0.028	−0.131	−0.193 to −0.068	<0.001
2b	−0.071	−0.182 to 0.039	0.202	−0.108	−0.186 to −0.030	0.007
3	−0.051	−0.153 to 0.050	0.317	−0.091	−0.159 to −0.024	0.008
HIRI						
1	0.138	0.031–0.244	0.012	0.099	0.024–0.174	0.010
2a	0.065	−0.032 to 0.165	0.184	0.000	−0.064 to 0.064	0.995
2b	0.046	−0.059 to 0.150	0.394	0.031	−0.045 to 0.107	0.418
3	0.021	−0.078 to 0.120	0.678	−0.022	−0.088 to 0.043	0.504

β-Values are standardized regression coefficients and represent the change in MISI and HIRI according to the low-grade inflammation score (LGI). Model 1 shows crude associations. Model 2a includes variables only mutually adjusted for HIRI or MISI, respectively. Model 2b includes variables only adjusted for age, sex, BMI, and waist-to-hip ratio. Model 3 includes variables from model 2b plus adjustment for HIRI or MISI, respectively. *LGI score with eight markers: IL-6, IL-8, TNF-α, SAA, sICAM, CRP, haptoglobin, and ceruloplasmin. #LGI score with six markers: IL-6, IL-8, TNF-α, SAA, sICAM, CRP.

the eight inflammatory genes that are included in the inflammation score were indeed higher in those with the muscle-IR than in those with no-IR (Supplementary Table 15). For three individual genes (*IL-6, sICAM, haptoglobin*), these differences were statistically significant. Such consistent upregulation of the inflammatory marker genes was not observed in adipose tissue of those with liver IR.

DISCUSSION

Here, we demonstrate distinct adipose tissue transcriptome profiles in tissue-specific IR. We show that an altered ECM gene expression profile in abdominal ScAT was present in overweight and obese individuals with pronounced hepatic IR. Furthermore, an inflammatory gene expression profile was particularly present in individuals with pronounced muscle IR and not with hepatic IR. We propose that an increased systemic inflammatory profile is a mechanism linking the increased expression of inflammatory genes in abdominal ScAT to muscle IR. In line with this, in two independent human cohorts, we show a relation between the combined score of plasma markers of low-grade inflammation and muscle IR, but not liver IR. Although the relationship between adipose tissue inflammation and IR has previously been posed (8), the findings in the present study extend these previous observations by indicating the tissue-specific nature of this relationship.

Increased abdominal ScAT inflammation appeared to be a predominant phenotype in muscle-IR individuals. This was mainly determined by upregulation of genes involved in chemotaxis, complement activation, and immune cell function related to lysosomes (e.g., cathepsins) and ubiquitin-proteasome. In recent years, several chemokines have been reported to be of importance in the etiology of obesity-associated inflammation and IR (31). Chemokines are crucial for the attraction of leukocytes from the circulation into tissues, including macrophages and T cells. For instance, it is known that higher total leukocyte counts precede and predict the incident risk of type 2 diabetes (32). Additionally, overrepresentation of T-cell–recruiting and –activating genes is of interest, given the recent implication of T-cell recruitment in obesity-related adipose tissue inflammation and IR in animal models (33) and humans (34), although T-cell infiltration in humans is much less characterized (35).

Furthermore, the upregulation of lysosomal genes such as cathepsins, and genes in the ubiquitin-proteasome pathway by which many intracellular proteins are degraded, is in line with the findings of previous studies and may point toward increased removal of apoptotic adipocytes (36). Moreover, complement factors (e.g., *C1Q*) are known to enhance phagocytosis by linking apoptotic cells and phagocytes, and contribute to the rapid clearance of dead cells (37). Notably, cell death is associated with increased immune cell infiltration (e.g., macrophages) and local tissue inflammation (38). Strong upregulation of ScAT *C1Q* is consistent with previous reports on ScAT gene expression in humans (19,39–42). *C1Qa* knockout mice were protected from high-fat diet–induced adipose tissue inflammation, systemic glucose intolerance, and hepatic IR (43). In addition, obesity-related adipocyte death was slightly increased in *C1Qa* knockout mice, implying that a reduction in the efficacy of clearing dead adipocytes may reduce macrophage inflammatory activation (43).

Although ScAT inflammation has been posed as a central factor in the development of IR, our data show for the first time that a ScAT inflammatory gene expression profile is most pronounced in the muscle-IR phenotype. Secretion media derived from ScAT explants of obese individuals have been shown to impair insulin signaling in both human myotubes (44,45) and hepatocytes (44). Furthermore, intracellular organelles like inflammasomes and autophagosomes in ScAT have been recognized in organ crosstalk and IR, albeit in indirect and incompletely understood ways (46).

The fact that we only found a relationship between ScAT inflammatory gene expression and muscle IR, not liver IR, might be related to a differential in vivo blood supply to both tissues. The liver may be more strongly affected by portal vein supply and factors derived from the visceral adipose tissue and the gut, while peripheral tissues like skeletal muscle might be more affected by the peripheral circulation. Indeed, as ScAT drains more systemically, this could affect skeletal muscle IR more than hepatic IR.

We hypothesized that increased ScAT inflammatory gene expression, as observed in the muscle-IR group, may lead to the secretion of proinflammatory adipokines in the circulation and a systemic proinflammatory profile inducing subsequently peripheral insulin sensitivity. In line with the adipose tissue transcriptome data, in two comparable cohorts, CODAM and the Maastricht Study, we showed that low-grade inflammation scores of plasma inflammatory markers were inversely associated with muscle insulin sensitivity (MISI), while we did not observe an association between the systemic low-grade inflammation score and hepatic IR (HIRI). These data provide support for the hypothesis that the link between an inflammatory ScAT gene expression profile, as found in DiOGenes, may translate into an increased systemic inflammatory profile, thereby explaining the link with peripheral insulin sensitivity.

In individuals with liver IR, increased ECM remodeling in abdominal ScAT was a predominant phenotype in the present study. The upregulation of genes related to ECM organization in ScAT is in line with the previously reported increased accumulation of ECM components in dysfunctional adipose tissue in obesity, which may decrease ECM flexibility and reduce adipose tissue plasticity by triggering adipocyte necrosis (47). In general, abnormal collagen deposition is tightly associated with increased local inflammation, characterized by infiltration by macrophages and other immune cells (48). Nevertheless, we did not observe a significant upregulation of ScAT inflammatory genes in individuals with liver IR compared with no-IR individuals. One explanation may be that our ScAT transcriptome data might reflect simultaneous processes related to ECM remodeling and fibrosis in the liver, which could in turn contribute to hepatic IR. Indeed, it has been shown that hepatic IR is also closely associated with increased ECM remodeling and fibrosis in the liver (49).

In this study, we were able to include large independent human data sets from DiOGenes and cohort studies (CODAM, the Maastricht Study). This included adipose tissue transcriptome analysis by RNA sequencing as well as detailed human phenotyping. The data from the multiple 5- to 7-point OGTTs, with glucose and insulin concentrations available, made it feasible to derive tissue-specific IR phenotypes (16,24,50). The estimated MISI and HIRI from OGTT results have been validated against gold standard hyperinsulinemic-euglycemic clamp studies (24) and have been used previously in large cohort and intervention studies (16,50). Nevertheless, contrary to standardized clamp-derived insulin sensitivity measures, MISI and HIRI may to some extent be determined by other biological processes such as the rate of glucose absorption as well as the incretin response. In addition, our data are adjusted for sex and body composition and they show robust and consistent associations between tissue-specific IR, adipose tissue transcriptome profiles, and systemic low-grade inflammation. A limitation of this study is that we do not have data regarding gene expression in visceral adipose tissue, as previous studies reported strong associations between hepatic IR and visceral adipose tissue (5).

To our knowledge, this study is the first to link the adipose tissue transcriptome with tissue-specific IR in a large population of overweight and obese individuals. These data open new and exciting avenues showing distinct tissue-specific IR phenotypes related to the development of type 2 diabetes and cardiovascular disease in overweight and obese individuals. Our findings of differential adipose tissue transcriptome and systemic inflammatory profiles in tissue-specific IR may provide targets and biomarkers for more tailored nutritional or pharmacological interventions in the prevention or treatment of cardiometabolic disease. Indeed, there is evidence from post hoc analyses that the response to nutritional intervention may depend on IR phenotype, e.g., being more insulin resistant at the level of the liver or skeletal muscle (16). Future studies are urgently warranted in order to obtain detailed insight into these differential metabolic phenotypes as well as related biomarkers.

Funding. This study was supported through a grant from the Maastricht University Medical Center+ and the Nestlé Institute of Health Sciences, Lausanne, Switzerland. DiOGenes was supported by the European Commission, Food Quality and Safety Priority of the Sixth Framework Program (FP6-2005-513946). The Maastricht Study was supported in part by the European Regional Development Fund via OP-Zuid, the Province of Limburg, the Dutch Ministry of Economic Affairs (grant 310.041), Stichting De Weijerhorst (Maastricht, the Netherlands), and the Pearl String Initiative Diabetes (Amsterdam, the Netherlands). The Maastricht Study was supported by the Cardiovascular Center (Maastricht, the Netherlands), the School for Cardiovascular Diseases (CARIM), the Care and Public Health Research Institute, School for Nutrition and Translational Research in Metabolism (Maastricht, the Netherlands), Stichting Annadal (Maastricht, the Netherlands), and Health Foundation Limburg (Maastricht, the Netherlands). The initiation of CODAM was supported by grants of the Netherlands Organisation for Scientific Research (940-35-034) and the Dutch Diabetes Research Foundation (98.901).

Duality of Interest. W.H.M.S. has received research support from several food companies, including Nestlé, DSM, Unilever, Nutrition et Santé, and Danone, and pharmaceutical companies such as GlaxoSmithKline, Novartis, and Novo Nordisk, and is an unpaid scientific advisor for the International Life Science Institute (ILSI) and ILSI Europe. A.A. has received grants and personal fees from Gelesis; personal fees from Acino International, BioCare Copenhagen, the Dutch Beer Institute, Groupe Éthique et Santé, IKEA Food Scientific Health Advisory Board, McCain Foods Ltd, Navamedic, Novo Nordisk, Denmark, Pfizer, Saniona, W International, Zaluvida; and grants from DC-Ingredients, outside the submitted work. A.V. is a full-time employee at the Nestlé Institute of Health Sciences SA. E.E.B. receives grant support from food industry companies such as DSM, Danone, Friesland Campina, Avebe, and Sensus, partly within the context of public-private consortia, has received funding from pharmaceutical companies such as Novartis,

and is involved in several task forces and expert groups related to the ILSI and ILSI Europe. No other potential conflicts of interest relevant to this article were reported.

Author Contributions. B.W.v.d.K. wrote the manuscript. B.W.v.d.K. and M.K. performed the transcriptomics and statistical analyses. B.W.v.d.K., M.K., M.A., M.M.J.v.G., N.V., W.H.M.S., A.A., A.V., D.L., C.J.H.v.d.K., S.J.P.M.E., C.G.S., C.D.A.S., G.H.G., I.C.W.A., J.W.E.J., C.T.E., and E.E.B. revised the manuscript and read and approved the manuscript for publication. B.W.v.d.K., M.K., M.A., M.M.J.v.G., N.V., C.J.H.v.d.K., C.D.A.S., G.H.G., I.C.W.A., J.W.E.J., C.T.E., and E.E.B. interpreted data. M.A., M.M.J.v.G., and N.V. supervised the statistical analyses. M.A. and J.W.E.J. supervised the transcriptomics analyses. M.M.J.v.G., C.J.H.v.d.K., S.J.P.M.E., C.G.S., and C.D.A.S. designed or contributed to data acquisition in CODAM and the Maastricht Study. W.H.M.S. and A.A. designed the DiOGenes clinical study. A.V. and D.L. performed RNA sequencing analysis. I.C.W.A., C.T.E., and E.E.B. designed and led the current study. C.T.E. and E.E.B. are the guarantors of this work and, as such, had full access to all the data in the study and take responsibility for the integrity of the data and the accuracy of the data analysis.

References

1. Ng M, Fleming T, Robinson M, et al. Global, regional, and national prevalence of overweight and obesity in children and adults during 1980-2013: a systematic analysis for the Global Burden of Disease Study 2013. Lancet 2014;384:766–781
2. Van Gaal LF, Mertens IL, De Block CE. Mechanisms linking obesity with cardiovascular disease. Nature 2006;444:875–880
3. Kahn SE, Hull RL, Utzschneider KM. Mechanisms linking obesity to insulin resistance and type 2 diabetes. Nature 2006;444:840–846
4. Goossens GH. The metabolic phenotype in obesity: fat mass, body fat distribution, and adipose tissue function. Obes Facts 2017;10:207–215
5. Klöting N, Blüher M. Adipocyte dysfunction, inflammation and metabolic syndrome. Rev Endocr Metab Disord 2014;15:277–287
6. Hoffstedt J, Arner E, Wahrenberg H, et al. Regional impact of adipose tissue morphology on the metabolic profile in morbid obesity. Diabetologia 2010;53: 2496–2503
7. Goossens GH, Blaak EE. Adipose tissue dysfunction and impaired metabolic health in human obesity: a matter of oxygen? Front Endocrinol (Lausanne) 2015;6:55
8. Kwon H, Pessin JE. Adipokines mediate inflammation and insulin resistance. Front Endocrinol (Lausanne) 2013;4:71
9. McArdle MA, Finucane OM, Connaughton RM, McMorrow AM, Roche HM. Mechanisms of obesity-induced inflammation and insulin resistance: insights into the emerging role of nutritional strategies. Front Endocrinol (Lausanne) 2013;4:52
10. Stinkens R, Goossens GH, Jocken JWE, Blaak EE. Targeting fatty acid metabolism to improve glucose metabolism. Obes Rev 2015;16:715–757
11. Stefan N, Fritsche A, Schick F, Häring H-U. Phenotypes of prediabetes and stratification of cardiometabolic risk. Lancet Diabetes Endocrinol 2016;4:789–798
12. Blaak EE. Characterisation of fatty acid metabolism in different insulin-resistant phenotypes by means of stable isotopes. Proc Nutr Soc 2017;76:419–424
13. Goossens GH, Moors CC, Jocken JW, et al. Altered skeletal muscle fatty acid handling in subjects with impaired glucose tolerance as compared to impaired fasting glucose. Nutrients 2016;8:164
14. Bird SR, Hawley JA. Update on the effects of physical activity on insulin sensitivity in humans. BMJ Open Sport Exerc Med 2017;2:e000143
15. Zheng J, Woo S-L, Hu X, et al. Metformin and metabolic diseases: a focus on hepatic aspects. Front Med 2015;9:173–186
16. Blanco-Rojo R, Alcala-Diaz JF, Wopereis S, et al. The insulin resistance phenotype (muscle or liver) interacts with the type of diet to determine changes in disposition index after 2 years of intervention: the CORDIOPREV-DIAB randomised clinical trial. Diabetologia 2016;59:67–76
17. Keller MP, Attie AD. Physiological insights gained from gene expression analysis in obesity and diabetes. Annu Rev Nutr 2010;30:341–364
18. Elbein SC, Kern PA, Rasouli N, Yao-Borengasser A, Sharma NK, Das SK. Global gene expression profiles of subcutaneous adipose and muscle from glucose-tolerant, insulin-sensitive, and insulin-resistant individuals matched for BMI. Diabetes 2011;60:1019–1029
19. Soronen J, Laurila P-P, Naukkarinen J, et al. Adipose tissue gene expression analysis reveals changes in inflammatory, mitochondrial respiratory and lipid metabolic pathways in obese insulin-resistant subjects. BMC Med Genomics 2012;5:9
20. Armenise C, Lefebvre G, Carayol J, et al. Transcriptome profiling from adipose tissue during a low-calorie diet reveals predictors of weight and glycemic outcomes in obese, nondiabetic subjects. Am J Clin Nutr 2017;106:736–746
21. Larsen TM, Dalskov S-M, van Baak M, et al.; Diet, Obesity, and Genes (Diogenes) Project. Diets with high or low protein content and glycemic index for weight-loss maintenance. N Engl J Med 2010;363:2102–2113
22. Hertle E, van Greevenbroek MM, Arts IC, et al. Distinct associations of complement C3a and its precursor C3 with atherosclerosis and cardiovascular disease. The CODAM study. Thromb Haemost 2014;111:1102–1111
23. Schram MT, Sep SJS, van der Kallen CJ, et al. The Maastricht Study: an extensive phenotyping study on determinants of type 2 diabetes, its complications and its comorbidities. Eur J Epidemiol 2014;29:439–451
24. Abdul-Ghani MA, Matsuda M, Balas B, DeFronzo RA. Muscle and liver insulin resistance indexes derived from the oral glucose tolerance test. Diabetes Care 2007;30:89–94
25. Viguerie N, Montastier E, Maoret JJ, et al. Determinants of human adipose tissue gene expression: impact of diet, sex, metabolic status, and cis genetic regulation. *PLoS Genet* 2012;8:e1002959
26. Love MI, Huber W, Anders S. Moderated estimation of fold change and dispersion for RNA-seq data with DESeq2. Genome Biol 2014;15:550
27. Eden E, Navon R, Steinfeld I, Lipson D, Yakhini Z. GOrilla: a tool for discovery and visualization of enriched GO terms in ranked gene lists. BMC Bioinformatics 2009;10:48
28. Slenter DN, Kutmon M, Hanspers K, et al. WikiPathways: a multifaceted pathway database bridging metabolomics to other omics research. Nucleic Acids Res 2018;46:D661–D667
29. Wlazlo N, van Greevenbroek MMJ, Ferreira I, et al. Complement factor 3 is associated with insulin resistance and with incident type 2 diabetes over a 7-year follow-up period: the CODAM Study. Diabetes Care 2014;37:1900–1909
30. Tanenbaum ME, Stern-Ginossar N, Weissman JS, Vale RD. Regulation of mRNA translation during mitosis. eLife 25 August 2015;4.
31. Tourniaire F, Romier-Crouzet B, Lee JH, et al. Chemokine expression in inflamed adipose tissue is mainly mediated by NF-κB. *PLoS one* 2013;8: e66515
32. Vozarova B, Weyer C, Lindsay RS, Pratley RE, Bogardus C, Tataranni PA. High white blood cell count is associated with a worsening of insulin sensitivity and predicts the development of type 2 diabetes. Diabetes 2002;51:455–461
33. Guzik TJ, Skiba DS, Touyz RM, Harrison DG. The role of infiltrating immune cells in dysfunctional adipose tissue. Cardiovasc Res 2017;113:1009–1023
34. Goossens GH, Blaak EE, Theunissen R, et al. Expression of NLRP3 inflammasome and T cell population markers in adipose tissue are associated with insulin resistance and impaired glucose metabolism in humans. Mol Immunol 2012;50:142–149
35. Travers RL, Motta AC, Betts JA, Bouloumié A, Thompson D. The impact of adiposity on adipose tissue-resident lymphocyte activation in humans. Int J Obes (Lond) 2015;39:762–769
36. Jaishy B, Abel ED. Lipids, lysosomes, and autophagy. J Lipid Res 2016;57: 1619–1635
37. Trouw LA, Blom AM, Gasque P. Role of complement and complement regulators in the removal of apoptotic cells. Mol Immunol 2008;45:1199–1207
38. Kuroda M, Sakaue H. Adipocyte death and chronic inflammation in obesity. J Med Invest 2017;64:193–196
39. Pietiläinen KH, Naukkarinen J, Rissanen A, et al. Global transcript profiles of fat in monozygotic twins discordant for BMI: pathways behind acquired obesity. *PLoS Med* 2008;5:e51
40. van Greevenbroek MMJ, Ghosh S, van der Kallen CJH, Brouwers MCGJ, Schalkwijk CG, Stehouwer CDA. Up-regulation of the complement system in

subcutaneous adipocytes from nonobese, hypertriglyceridemic subjects is associated with adipocyte insulin resistance. J Clin Endocrinol Metab 2012;97:4742–4752
41. Das SK, Ma L, Sharma NK. Adipose tissue gene expression and metabolic health of obese adults. Int J Obes 2015;39:869–873
42. Wiklund P, Zhang X, Pekkala S, et al. Insulin resistance is associated with altered amino acid metabolism and adipose tissue dysfunction in normoglycemic women. Sci Rep 2016;6:24540
43. Hillian AD, McMullen MR, Sebastian BM, et al. Mice lacking C1q are protected from high fat diet-induced hepatic insulin resistance and impaired glucose homeostasis [published correction appears in J Biol Chem 2013;288:28308]. J Biol Chem 2013;288:22565–22575
44. Kranendonk MEG, Visseren FLJ, van Herwaarden JA, et al. Effect of extracellular vesicles of human adipose tissue on insulin signaling in liver and muscle cells. Obesity (Silver Spring) 2014;22:2216–2223
45. Sarr O, Strohm RJ, MacDonald TL, et al. Subcutaneous and visceral adipose tissue secretions from extremely obese men and women both acutely suppress muscle insulin signaling. Int J Mol Sci 2017;18. pii: E959
46. Indrakusuma I, Sell H, Eckel J. Novel mediators of adipose tissue and muscle crosstalk. Curr Obes Rep 2015;4:411–417
47. Sun K, Tordjman J, Clément K, Scherer PE. Fibrosis and adipose tissue dysfunction. Cell Metab 2013;18:470–477
48. Lin D, Chun T-H, Kang L. Adipose extracellular matrix remodelling in obesity and insulin resistance. Biochem Pharmacol 2016;119:8–16
49. Koyama Y, Brenner DA. Liver inflammation and fibrosis. J Clin Invest 2017;127:55–64
50. van der Kolk BW, Vogelzangs N, Jocken JWE, et al.; DiOGenes Consortium. Plasma lipid profiling of tissue-specific insulin resistance in human obesity. Int J Obes (Lond) 2019;43:989–998